Nanotube Formation and Surface Study of New Ternary Titanium Alloys

*H.C. Choe, Y.M. Ko, [1]W. A. Brantley

College of Dentistry, Chosun University, 2nd stage of Brain Korea 21 for College of Dentistry, Gwangju, Korea
[1]College of Dentistry, Ohio State University, Columbus, OH, USA
*hcchoe@chosun.ac.kr

ABSTRACT

New titanium alloys with improved biocompatibility have been developed for dental and biomedical applications. The osseointegration of implants depends on surface properties of these alloys, and the nature of the oxide film at the metal-oxide-bone. Also, stress acting on the interface between bone and implant can influence the bone resorption, due to stress-shielding effects. So we have tried to improve this effect by manufacture of new ternary alloy containing Ta, Nb, and Zr alloying elements. In this study, nanotube formation and surfaces of new ternary titanium alloys have been investigated using various electrochemical methods after anodizing on the Ti-30Ta-XZr and Ti-30Nb-XZr alloy surfaces, where X = 3 and 15 (wt %) The polarization resistance of nanotube-formed new ternary alloys was lower than that of the corresponding non-nanotube-formed alloy. The diameter and depth of the nanotubes could be controlled, depending upon the composition and titanium alloy phased for osseointegration of bio-implant.

Keywords: Nanotube, Corrosion, Polarization resistance, Ti-Ta-Zr, Ti-Nb-Zr alloy, Implant

1 INTRODUCTION

Pure titanium and its alloys are drastically used in implant materials due to their excellent mechanical properties, high corrosion resistance and good biocompatibility [1]. However, the widely used Ti-6Al-4V is found to release toxic ions (Al and V) into the body, leading to undesirable long-term effects. Ti-6Al-4V has much higher elastic modulus (100-120GPa) than cortical bone (10-30 GPa) [1]. Therefore, titanium alloys with low elastic modulus have been developed as biomaterials to minimize stress shielding [2].

Recently, Ti-Nb and Ti-Ta based alloy systems have been studied and found to display both lower elastic moduli and higher tensile strengths than are common for metals and alloys. Nb, and Ta can be stabilized to β-phase of Ti alloy and β-phase structure exhibits about 60-80 GPa of Young's modulus [1]. Some researcher reported that the Ti-30%Ta alloy with martensite α"-phase has the potential to become a new candidate for biomedical application due to its good combination of low modulus and high strength. To improve bone tissue integration on implant surfaces, various techniques have been used to increase the roughness of the implant surfaces [3]. Cell adhesion and proliferation depend on surface roughness [4] and metal ion dissolution [5]. The electrochemical formation of novel highly ordered oxide nanotube layers has been reported for Ti anodization in fluoride-containing acid electrolytes at moderate voltage[6]. Nanotube formation on the Ti oxide is important to improve the cell adhesion and proliferation in clinical use. It is possible to control nanotube size and morphology for biomedical implant use. Factor is applied voltage, alloying element, current density, time, and electrolytes. Recently, many results of nanotube formation have been reported on effects of these factors without consideration of alloying element in ternary alloys,

In this study, nanotube formation and surface characteristics of Ti-30Nb-xZr and Ti-30Ta-xNb alloy with low elastic modulus have been investigated using various electrochemical methods.

2 MATERIALS AND METHODS

Ternary Ti-30Nb-xZr(x=3,15wt%) and Ti-30Ta-xNb (x=3,15wt%) alloys were prepared by using high purity sponge Ti (G&S TITANIUM, Grade. 4, USA), Ta, Zr and Nb sphere (Kurt J. Lesker Company, 99.95% wt.% in purity). Two kinds of Ti alloys prepared using the vacuum arc melting furnace. The weighed charge materials were prepared by the vacuum arc furnace, under the purified Ar gas into water cooling copper hearth chamber in vacuum atmosphere of 10^{-3}torr, and controlled atmosphere in chamber by method to keep vacuum again. Also, before melting, the constituents were cleaned with methanol to minimize oxygen quantity and surface contaminants in chamber and pure Ti was melted six times with purified argon gas. After that, melting treatment was carried out more than six times by reversing the alloy sponges in order to homogenize, and each time was held in the molted state for 5 min. in a high purity argon atmosphere by arc furnace with water-cooled copper hearth and solution treatment was carried out for 1hr at 1050°C in an argon atmosphere, followed by water quenching to stabilize the β phase

Microstructures of the alloys were examined by optical microscopy (OM, OLYMPUS BM60M, JAPAN) and scanning electron microscopy (SEM, HITACHI-3000, JAPAN). The specimens for the OM and SEM analysis were etched in Keller's solution consisting of 2 ㎖ HF, 3 ㎖ HCl, 5 ㎖ HNO_3 and 190 ㎖ H_2O.

Nanotube formation was carried out with a conventional three-electrode configuration with a platinum counter electrode and a saturated calomel (SCE) reference electrode. Experiments were performed in 1M H_3PO_4 with small additions of NaF(0.8wt%). All experiments were conducted at room temperature. Electrochemical treatments were performed by using potentiostat (EG&G Co, 362, U.S.A). The electrochemical treatment consisted of a potential ramp from the open-circuit potential (*E*ocp) to an end potential at 10 V with a scan rate of 500mV/s followed by holding the sample at 10V for 2h.

In order to investigate the corrosion behavior, potentiostatic test was carried out using a potentiostat(EG&G PARSTAT 2273) test at constant potential 300 mV in 0.9% NaCl solution at 36.5±1℃. Electrochemical impedance spectroscopy was performed (10 mHz to 100 kHz) in 0.9% NaCl solution at 36.5±1℃. All electrochemical characteristics were performed in a standard three-electrode cell having specimen as a working electrode and a high carbon as counter electrode. The potential of working electrode was measured against a saturated calomel electrode (SCE) and all given potentials were referred to this electrode. After electrochemical corrosion tests, the surfaces of each specimen were investigated by using FE-SEM.

3 RESULT AND DISCUSSION

Fig. 1 is FE-SEM micrographs showing the microstructure of homogenized Ti alloy surface. Figure 1(a) and (b) show the microstructure of Ti-30Ta-3Zr and Ti-30Ta-15Zr. Figure 1(c) and (d) show the microstructure of Ti-30Nb-3Zr and Ti-30Nb-15Zr alloy, respectively. The microstructures of the Ti-30Ta-xZr alloys had a needle-like appearance. And the thick of needle like -α structure increased as Zr content increased. It is confirmed that Zr content played a role to stabilizer of α phase[7]. The quenched alloys exhibit the lamellar martensite α' structure at below 20wt% Ta, and exhibit the needle-like orthorhombic martensite α" structure from 30 to 50wt% Ta. We confirmed that the microstructure changes from α phase to β-phase through XRD and β phase increases, as Nb content increases[7]. With these results, we could make an analogical inference that Nb and Ta is the β stabilizing element as the β-phase increases according to the addition of Nb and Ta. The literature reports that the amount of needle-like orthorhombic martensite α" structure increases with increasing cooling rate due to the transformation of β phase into α" phase[8].

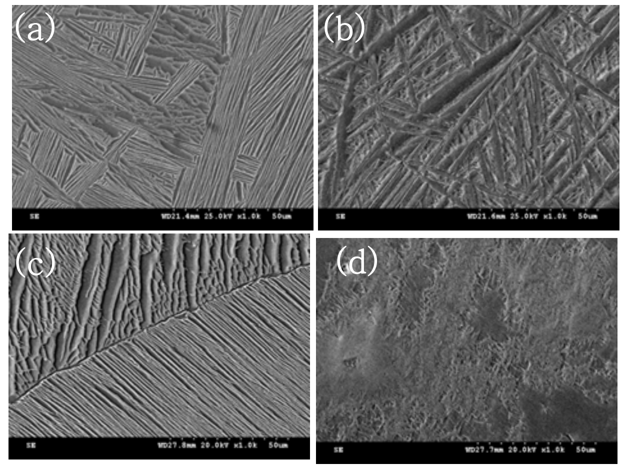

Fig. 1. FE-SEM micrographs of homogenized Ti-30Ta-xZr and Ti-30Nb-xZr alloys.
(a) Ti-30Ta-3Zr (b) Ti-30Ta-15Zr
(c) Ti-30Nb-3Zr (d) Ti-30Nb-15Zr

Fig. 2 shows the evolution of TiO_2 nanopores grown from Ti films in 1M H_3PO_4 + 0.8wt% NaF electrolyte solution for 2h at an applied anodic potential of 10V. . Figure 2(a) and (b) show the nanotube morphology of Ti-30Ta-3Zr and Ti-30Ta-15Zr. Figure 2(c) and (d) show the nanotube morphology of Ti-30Nb-3Zr and Ti-30Nb-15Zr alloy, respectively. Nanotube formed in β phase showed the regular array with pore diameters around 150nm and the wall thickness in the range of 20nm and 100nm interspace of nanotube, but nanotube formed in α phase showed irregular array with small(50nm) and large diameter(200nm) of nanotube. It can be concluded that α phase has Zr rich with martensite α" structure and high stress energy in matrix. Consequently, and stable nanotube can be formed in β phase compared to α phase. Small and large nanotube morphplogy showed predominantly in case of increasing Zr content to β phase.

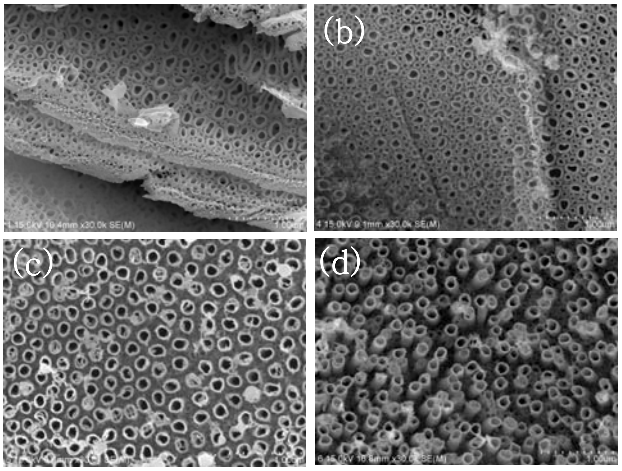

Fig. 2. FE-SEM image of Ti-Nb-Zr alloy nanotube layer formed in 1M H_3PO_4 + NaF(0.8wt%) for 2h at 10V.
(a) Ti-30Ta-3Zr (b) Ti-30Ta-15Zr (c) Ti-30Nb-3Zr, (d) Ti-30Nb-15Zr

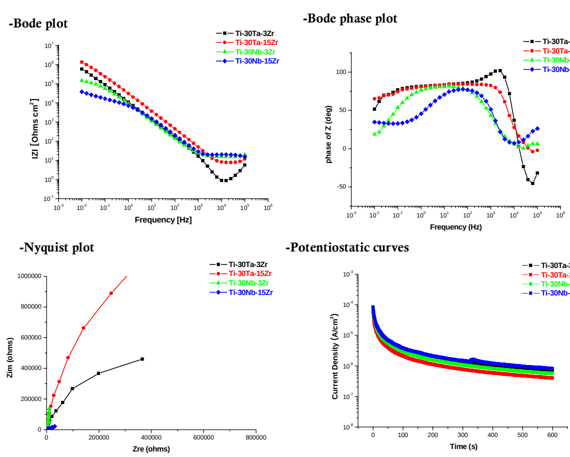

Fig. 3. AC impedance and potentistatic results of non-nanotube formed surface in in 0.9% NaCl solution at 36.5±1℃. (a) Bode plot, (b) Bode-phase plot, (c) Nyquist plot, (d) Potentiostatic curves

The polarization resistance(R_p)of non-nanotube formed alloy is higher than that of nanotube formed alloy. From impedance tests of non-nanotubed alloys, the polarization resistance of Ti-30Ta-3Zr alloy was higer than that of Ti-30Nb-xZr alloy, whereas, in case of nanotubed alloys, the polarization resistance of Ti-30Nb-3Zr alloy was higer than that of other alloy. Zr additions to Ti-30Nb alloy have improved electrochemical corrosion behavior due to nobler characteristics to the alloys [8]. The polarization resistance of nanotubed alloy was lower than that of non-nanotubed alloy as shown in Table 1. It was considered that nanotubed surface has unstable surface due to amorphous structure without heat treatment for crystallinity. Amorphous structure is easily dissolved in halides ion contained electrolytes [9]. The high value of R_p implies a high corrosion resistance of alloy, that is, a low rate of released metallic ion into the electrolytic solution or nanotube on the surface. The Bode plot results indicated that the corrosion behavior of alloy in solution was under charge-transfer controlled because of the local variation of aggressive ion like Cl^-, preferentially attacking or damaging the oxide film and nanotube. The Bode plots for all the alloys before nanotube formation showed near capacitive response in the high and middle frequency region. The Bode plots for all the alloys after nanotube formation showed near capacitive response in the lower and middle frequency region which was characterized by slope≈ -1 in the log|z| vs. log(f) curve. It seems that the alloying element has been responsible for the resulting better corrosion resistance of nanotubed Ti-30Ta-xZr alloy and Ti-30Nb-xZr alloy. From potentiostatic test, surface stability (current density vs time) of nanotubed alloy showed the lower than that of non-nanotubed alloy without Ti-30Nb-3Zr alloy.

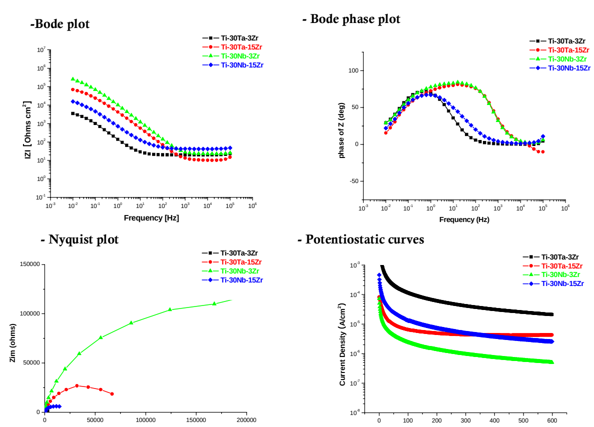

Fig. 4. AC impedance and potentistatic results of nanotube formed surface in in 0.9% NaCl solution at 36.5±1℃. (a) Bode plot, (b) Bode-phase plot, (c) Nyquist plot, (d) Potentiostatic curves

Table 1. EIS parameters of non-nanotubed and nanotubed Ti-Ta-Zr and Ti-Nb-Zr alloys.

Non treatment	Ti-30Ta-3Zr	Ti-30Ta-15Zr	Ti-30Nb-3Zr	Ti-30Nb-15Zr
Rp (Ω ㎠)	5.87×10^5	1.35×10^6	1.46×10^5	3.77×10^4
Rs (Ω ㎠)	0.873	7.6575	15.225	15.53
Nanotube formed	Ti-30Ta-3Zr	Ti-30Ta-15Zr	Ti-30Nb-3Zr	Ti-30Nb-15Zr
Rp (Ω ㎠)	3.49×10^3	6.93×10^4	2.53×10^5	1.56×104^4
Rs (Ω ㎠)	19.756	10.103	22.686	41.874

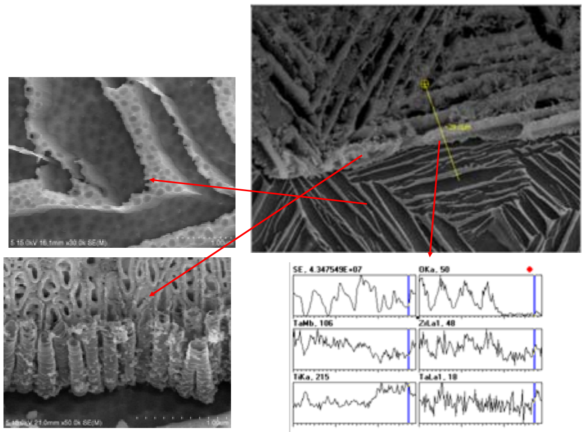

Fig. 5. FE-SEM image and line profiles of Ti-30Nb-3Zr alloy nanotube layer formed in 1M H_3PO_4 + NaF(0.8wt%) for 2h at 10V after potentiostatic corrosion test.

Fig. 5 shows FE-SEM image and line profiles of Ti-30Nb-3Zr alloy nanotube layer formed in 1M H_3PO_4 + NaF(0.8wt%) for 2h at 10V after potentiostatic corrosion test. Some nanotube morphology was changed from circle to parabolic style and tore off from tip of tube compared to non-corroded surface (Fig.2). From cross-section image shows pore tubes with many rings on their wall. This is that the regularity of the rings corresponds to the periodicity of current oscillations of current –time curves [10]. From line profile, Nb content in the nanotube covered region was slightly higher than that of uncovered region due to formation of Nb_2O_5 on the nanotube film.

4 CONCLUSIONS

The corrosion and polarization resistance of nanotube-formed new ternary alloys was lower than that of the corresponding non-nanotube-formed new ternary alloy.
The diameter and depth of the nanotubes could be controlled, depending upon the composition and titanium alloy phased for osseointegration of bio-implant.

ACKNOWLEDGEMENT

"This work was supported by research funds from 2nd stage of Brain Korea 21 for College of Dentistry"

REFERENCES

[1] G. He, M. Hagiwara, "Ti alloy design strategy for biomedical applications", Materials Science and Engineering, C 26, 14-19, 2006.

[2] D. Kuroda, M. Niiomi, "Design and mechanical properties of new β-type titanium alloys for implant materials", Materials Sci and Eng A, 243, 244, 2001.

[3] H.C. Choe, Y.M.Ko, W.A.Brantley, "Nano-Surface Behavior of Osteoblast Cell-Cultured Ti-30(Nb,Ta) with Low Elastic Modulus" NSTI-Nanotech-2007, 2, 744-747, 2007.

[4] K. Anselme, "Osteoblast adhesion on biomaterials", Biomaterials, 21, 667-681, 2000.

[5] T. Hanawa, "Metal ion release from metal implants", Matr. Sci. & Eng., 24, 745-752, 2004.

[6] V. Zwilling, M. Aucouturier, E. Darque-Ceretti, A. Boutry-Forveille, " Anodic oxidation of titanium and TA6V alloy in chromic media, An electrochemical approach," Electrochemi Acta, 45, 921-929, 1999.

[7] J. J. Park, H. C. Choe, Y.M. Ko, "Corrosion Characteristics of TiN and ZrN coated Ti-Nb alloy by RF-sputtering", Materials Science Forum , 539-543, 1270-1275, 2007.

[8] D. Q. Martins, W. R. Osorio, M.E.P.Souza, R. Caram, A. Garcia, Electrochemica Acta, 53, 2809-2817, 2008.

[9] H.C. Choe, Y.M.Ko, S.S.Kim, W.A.Brantley, "Surface Characteristics of Tooth Ash Coatrings on Ti and Ti-6Al-4V Deposited by Pulsed Laser Method", AEPSE2007, NSTI-Nanotech-2007, 41, 2007.

[10] Jan M. Macak, K. Sirotna, P. Schmuki, "Self-organized porous titanium oxide preparaed in Na2SO4/NaF electrolytes", Electrochemical Acta, 50, 3679-3684, 2005.